# EFFECTS OF PRIMARY RECOIL ENERGY ON THE PRODUCTION RATE OF MOBILE DEFECTS DURING ELEVATED TEMPERATURE IRRADIATION*

P. R. Okamoto, L. E. Rehn and R. S. Averback
Materials Science and Technology Division
Argonne National Laboratory
Argonne, Illinois  60439

FINAL

November 1984

## DISCLAIMER

MASTER

# EFFECTS OF PRIMARY RECOIL ENERGY ON THE PRODUCTION RATE OF MOBILE DEFECTS DURING ELEVATED TEMPERATURE IRRADIATION*

P. R. Okamoto, L. E. Rehn and R. S. Averback
Materials Science and Technology Division
Argonne National Laboratory
Argonne, Illinois 60439

## ABSTRACT

Radiation-induced segregation rates in a Ni-12.7 at.% Si alloy have been measured as a function of temperature using ions of various masses and energies. An analysis of the segregation kinetics using a simple analytical model yielded the relative efficiency of each of the ions for producing mobile defects directly from ratios of their measured segregation rates. In this paper, we also show that the relative efficiencies can also be determined from measured shifts in the peak segregation temperature. Both methods yield a strong decrease in efficiency with increasing ion mass. The reduction in efficiency for the heavior ions was found to be significantly larger than that measured at very low temperatures by resistivity techniques. The latter are often used as a basis for correlating damage structures produced at elevated temperatures. Differences between the low and high temperature measurements indicate that relative efficiencies determined from segregation measurements are more reliable for correlating microstructural changes that are produced in different irradiation environments at high temperatures.

# EFFECTS OF PRIMARY RECOIL ENERGY ON THE PRODUCTION RATE OF MOBILE DEFECTS DURING ELEVATED TEMPERATURE IRRADIATION*

P. R. Okamoto, L. E. Rehn and R. S. Averback
Materials Science and Technology Division
Argonne National Laboratory
Argonne, Illinois  60439

## 1.  Introduction

Despite its greater technological importance, less is known about defect production mechanisms at elevated temperatures then is known at very low temperatures.  For predicting microstructural changes at elevated temperatures, the quantity of interest is the rate of production of mobile defects.  Due to defect interactions within cascades, the net production rate of mobile defects can be only a small fraction of the calculated atomic displacement rate (dpa/s) which is commonly used to correlate damage structures produced by different irradiation particles.  Hence the production efficiency for mobile defects must be known as a function of the irradiation species and energy before quantitative correlations between different irradiation environments can be made.

Recently, Okamoto et al., [1] proposed a method for determining the relative efficiencies of different particles directly from ratios of measured segregation rates of Si in irradiated Ni-Si alloys.  Here it is shown that the relative efficiencies can also be obtained from measured shifts in the peak segregation temperature.  Efficiencies obtained by these methods from measurements of radiation-induced segregation in a Ni-12.7 at.% Si alloy are in good agreement with those obtained by computer fitting techniques.  A detailed account of the experimental measurements and analysis can be found in Ref. 2.

---

## 2. Method of Analysis

When Ni-Si alloy are irradiated at elevated temperatures, preferential transport of Si by defect fluxes toward the surface results in the formation and growth of $Ni_3Si$ surface coatings [3]. Previous work [4-6] has shown that the coatings obey parabolic growth kinetics, i.e., the coating thickness, W, as a function of irradiation time t is given by

$$W(t) = At^{1/2} \qquad (1)$$

where A is the growth-rate constant expressed in units of $length/(time)^{1/2}$. The growth constant provides a simple quantitative measure of the segregation rate induced by the irradiation. As shown by Okamoto et al., [1], the temperature and dose-rate dependences of the growth constant can be exploited to obtain information about the production efficiencies of ions for producing mobile defects. Details of the coating growth model and the original analysis for extracting such information is given in Ref. 1. Here we focus on the additional information contained in the dose-rate dependence of the peak segregation temperature.

The model assumes that coating growth is controlled by the diffusion of tightly bound Si-interstitial (s-i) complexes toward the surface. Except in a Si depleted zone immediately beneath the surface coating, quasi-steady-state conditions for vacancies and s-i complexes are assumed during coating growth. According to the model, the growth-rate constant expressed in units of $length/(dose)^{1/2}$, is given by

$$A_K \equiv \frac{A}{K_c^{1/2}} = \left[ \frac{2c_s^o}{c_s^P(c_s^P - c_s^o)} \right]^{1/2} \cdot \left( \frac{D_{is}C_{is}}{K_c} \right)^{1/2} \qquad (2)$$

where $K_c$ is the calculated atomic displacement rate, $C_s^o$ is the bulk Si concentration, $C_s^p$ is the concentration of Si in the surface coating, $D_{1s} = (2/21)\, a_o^2\, \nu_{1s}$ is the diffusion coefficient of the s-i complexes, $a_o$ is the lattice parameter, $\nu_{1s}$ is the jump frequency of the s-i complexes, and $C_{1s}$ is their steady-state bulk concentration immediately behind the Si depleted zone.

By use of conventional rate theory [7], it has been shown [1] that

$$\frac{D_{1s}C_{1s}}{K_c} = \frac{2}{21}\, a_o^2\, (\frac{\epsilon}{P_1})\, S(\eta, \beta) \tag{3}$$

where $\epsilon = K_o/K_c$ is the production efficiency for mobile defects, $K_o$ is the actual production rate of mobile defects, and $P_1$ is the total sink annihilation probability for interstitials. $S(\eta, \beta)$ is the fraction of defects annihilating at sinks and is given by [1]

$$S(\eta, \beta) = \frac{2}{\eta}\, (1 + \beta) \left\{ [1 + \frac{\eta}{(1 + \beta)^2} ]^{1/2} - 1 \right\} \tag{4}$$

where

$$\eta = \frac{4a_r(\nu_v + \frac{1}{7}\, \nu_{1s})}{\nu_v \nu_{1s} P_v P_1} \quad , \quad \beta = \frac{a_r(\nu_v + \frac{1}{7}\, \nu_{1s})\, \tilde{C}_v}{\nu_{1s} P_1} \tag{5}$$

In Eq. (5), $a_r$ is the number of lattice sites in the recombination volume for vacancies and s-i complexes, $\nu_v = \nu_v^o \exp(-H_v^m/kT)$ is the vacancy jump frequency, $\nu_v^o$ is the jump attempt frequency, $H_v^m$ is the vacancy migration energy, $\bar{C}_v = \exp(S_v^F/k)\exp(-H_v^F/kT)$ is the average thermal-equilibrium concentration of vacancies, $S_v^F$ is the vacancy entropy of formation, $H_v^F$ is the vacancy formation energy, and $P_v$ is the total sink annihilation probability for vacancies.

Internal friction studies [8] indicate that s-i complexes are considerably more mobile than vacancies ( $D_{is} \gg D_v$ ). For this condition, it has been shown [1] that at low temperatures where defects are annihilated mainly by recombination,

$$A_K = \frac{2}{3} \left[ \frac{2C_s^o}{C_s^P(C_s^P - C_s^o)} \right]^{1/2} \left[ \frac{a_o^2 \epsilon D_v}{a_r K_c} \right]^{1/4} \tag{6}$$

and at high temperatures where $\eta \ll (1 + \beta)^2$,

$$A_K = \frac{2}{3} \left[ \frac{2C_s^o}{C_s^P(C_s^o - C_s^o)} \right]^{1/2} \left[ \frac{a_o^2 \epsilon}{a_r \bar{C}_v} \right]^{1/2} \tag{7}$$

These solutions are sketched in Fig. 1 for the case $\epsilon = 1$. They show that the apparent activation enthalpy of the growth-rate constant is equal to $H_v^m/4$ at low temperatures, and to $H_v^F/2$ at high temperatures. Equation (6) also shows that the growth-rate constant varies inversely with the 1/4 power of the calculated dose-rate at low temperatures, and is independent of dose-rate at high temperatures.

The temperatures dependence of the growth-rate constant is contained primarily in the sink annihilation fraction, $S(\eta, \beta)$. Hence the temperature $T_m$ at which the growth-rate constant is a maximum will be given approximately by the temperature at which $dS/d(1/kT) = 0$. To obtain an approximate analytical solution, the quantity $[1 + \eta/(1 + \beta)^2]^{1/2}$ in Eq. (4) can be expanded. Only the first four terms in the expansion are needed to define the peak. The solution for the case where $\eta \ll (1 + \beta^2)$ and $\beta^2 \gg 1$, i.e., when recombination is dominant over defect annihilation at sinks, is given approximately by

$$T_m = \frac{H_v^m + 2H_v^F}{k\ln\left[\dfrac{3a_r v_v^o \exp(2S_v^F/k)}{2\epsilon K_c}\left(\dfrac{H_v^F + M}{H_v^m - 2M}\right)\right]} \tag{8}$$

where

$$M = \frac{1}{P_1}\frac{dP_1}{d(1/kT)} \tag{9}$$

Equation (8) shows that for bombarding particles with identical efficiencies, the peak segregation temperature will increase with increasing calculated dose-rates. It also shows that for irradiations carried out at the same calculated dose-rates but with particles of different efficiencies, the more efficient particle will have the higher peak segregation temperature.

The factor M depends on the temperature dependence of the sink annihilation probability. Our own electron microscopy observations indicate that near the peak segregation temperature, the sink density is relatively low in the region of interest, namely less then a few tenths of a micron below the bombarded surface. However, at these relatively shallow depths the surface acts as a strong sink for defects. Hence for the present calculations, the surface will be assumed to be the dominant sink. As shown by Lam et. al., [9] the surfaces of a foil of thickness L are equivalent to a sink annihilation probability given by

$$P_1 = \frac{2}{21}a_o^2\left(\frac{12}{L^2} + \frac{3}{L}f_o^{1/4}\right) \tag{10}$$

where

$$f_o^{1/4} = (\frac{3a_r \varepsilon K_c}{a_o^2 \nu_v})^{1/4}$$ (11)

When the second term in Eq. (10) becomes the dominant term, i.e., for very thick foils, the defect concentration profiles approaches that for a semi-infinite medium. In this case, it can be seen from Eq. (9) and (11) that M becomes a constant equal to $H_v^m/4$, resulting in a decrease in $T_m$ relative to the case where $P_i$ is independent of temperature.

Before applying Eqs. (6), (7) and (8) to experimental data, it is important to note that the recombination volume parameter $a_r$ and the production efficiency factor, $\varepsilon$, always enter these equations as a ratio. Hence a unique value for the efficiency cannot be obtained by fitting experimental data unless $a_r$ is known. However, Eqs. (6), (7) and (8) can be used to determine the ratios or the relative efficiencies of two different particles (1 and 2) using only the known or measurable quantities, $A_k$, $K_c$, $H_v^m$, $H_v^F$, $T_m$, and T. From Eq. (6), the relative efficiencies in the low temperature recombination dominant region are given by

$$\frac{\varepsilon_1}{\varepsilon_2} = \frac{K_c^{(1)}}{K_c^{(2)}} \left[ \frac{A_K^{(1)}}{A_K^{(2)}} \right]^4 \exp \left[ - \frac{H_v^m}{K} (\frac{1}{T^{(2)}} - \frac{1}{T^{(1)}}) \right]$$ (12)

and from Eq. (7), in the higher temperature regime,

$$\frac{\varepsilon_1}{\varepsilon_2} = \left[ \frac{A_K^{(1)}}{A_K^{(2)}} \right]^2 \exp \left[ - \frac{H_v^F}{2} (\frac{1}{T^{(1)}} - \frac{1}{T^{(2)}}) \right]$$ (13)

In the intermediate temperature recombination dominant regime, Eq. (8) gives

$$\frac{\epsilon_1}{\epsilon_2} = \frac{K_c^{(2)}}{K_c^{(1)}} \exp\left[-\frac{(H_v^m + 2H_v^F)}{k}\left(\frac{1}{T_m^{(1)}} - \frac{1}{T_m^{(2)}}\right)\right] \qquad (14)$$

It is important to emphasize that the above equations are applicable only under irradiation conditions where mutual recombination is the dominant mode for defect annihilation.

## 3. Comparison with Experiment

In this section, the equations obtained in the previous section are applied to recent coating growth measurements obtained from a Ni-12.7 at.% Si alloy. Details of the experimental procedures and measurements are given in Ref. 2.

In Fig. (2), taken from Ref. 2, coating growth measurements carried out over the temperature range from 350 to 650°C are shown for six different irradiations. The results reveal that for particles of approximately the same energy, a large reduction in the growth-rate constant occurs with increasing ion mass. The He data exhibit the predicted [cf. Eq. (6)] inverse 1/4 power dependence of the growth-rate constant on dose-rate at lower temperatures, and no dependence on dose-rate at higher temperatures. A least squares fit yields apparent activation energies of 0.31 eV and 0.75 eV for the low and high temperature Arrhenius regions, respectively. It follows from Eqs. (6) and (7) that $H_v^m = 1.24$ eV and $H_v^F = 1.5$ eV. The He data also exhibit the shift [cf. Eq. (8)] in the peak segregation temperature to higher temperatures with increasing dose-rate, expected of particles of identical production efficiencies. A comparison of the proton and the lower dose-rate He data also show the expected shift to higher temperatures in the peak segregation

temperature of the more efficient particle, when irradiations using two different particles are carried out at the same calculated dose-rate.

Using Eq. (2), a computer fitting procedure was used to obtain "best fit" lines [cf. Fig. (2)] using the ratio ($\epsilon/a_r$) as the main fitting parameter. The sink annihilation probability given by Eq. (10) was employed in the calculations using L = 800 nm. The other parameters used in the calculations are: $H_v^m$ = 1.24 eV, $H_v^F$ = 1.5 eV, $S_v^F$ = 5 K, $v_v^o$ = 5 x $10^{13}$, $H_{1s}^m$ = 0.6 eV, and $a_o$ = 3.52 x $10^{-8}$cm. The ratios ($\epsilon/a_r$), relative efficiencies (relative to the 1-MeV H), and the peak segregation temperatures obtained from the best fit cases are listed in Table 1. The relative efficiencies and peak segregation temperature obtained from Eq. (14) and (8) are also listed.

As shown in Table 1, the peak segregation temperatures obtained from Eq. (8), and the relative efficiencies of different particles determined from the relative shift in their peak segregation temperatures are in good agreement with those obtained from the proton through Ni data using computer fitting techniques. This implies that mutual recombination was the dominant defect annihilation mode for these irradiations. On the other hand, the Kr data could not be fitted consistently either with Eq. (14) or with Eq. (2). This indicates that irradiation induced sinks comparable to or greater than the equivalent sink density of the surface were produced during the Kr irradiation, particularly at the lower temperatures. Therefore, the efficiency for Kr listed in Table 1 represents only a minimum value obtained by fitting data obtained at temperatures above 550 C.

The relative efficiencies normalized to the 1-MeV protons obtained for the best fit cases, are plotted in Fig. 3 as a function of the weighted-average recoil energy, $P_{1/2}$. $P_{1/2}$ is that primary recoil energy above and below which half the defects are produced. It is a measure of the spatial

distribution of the defect production. A detailed discussion of $P_{1/2}$ can be found in ref. 10. Figure 3, taken from Ref. 2, provides a quantitative representation of the relative efficiency for producing mobile defects as a function of the "hardness" of the primary recoil spectrum. The general shape of the curve is qualitatively similar to the curves of efficiency versus $P_{1/2}$ obtained by Averback et al. [10] who used electrical resistivity measurements to study defect production at very low temperatures in copper and silver over a wide range of recoil energies. However, there are significant quantitative differences. The resistivity measurements saturate at an efficiency which was still about 40% of that found at the lowest primary recoil energy. In contrast, the limiting value in Fig. 3 appears to be considerably less, i.e., only about 10% or less than that found at the lowest primary recoil energy.

It is important to recognize that the electrical resistivity changes measure the total number of stable defects which are introduced during irradiation, whereas the coating-growth measurements are sensitive only to those mobile defects which participate in long range atom transport, i.e., only some fraction of the total monitored by resistivity changes. The quantitative difference is also of technological significance. Defect production efficiencies obtained at very low temperatures are often used as a basis for correlating microstructural changes induced by different bombarding particles at elevated temperatures. However, the fact that quantitative differences exist suggests that the relative efficiencies determined from coating-growth measurements offer a more reliable basis for correlating radiation effects induced at elevated temperatures.

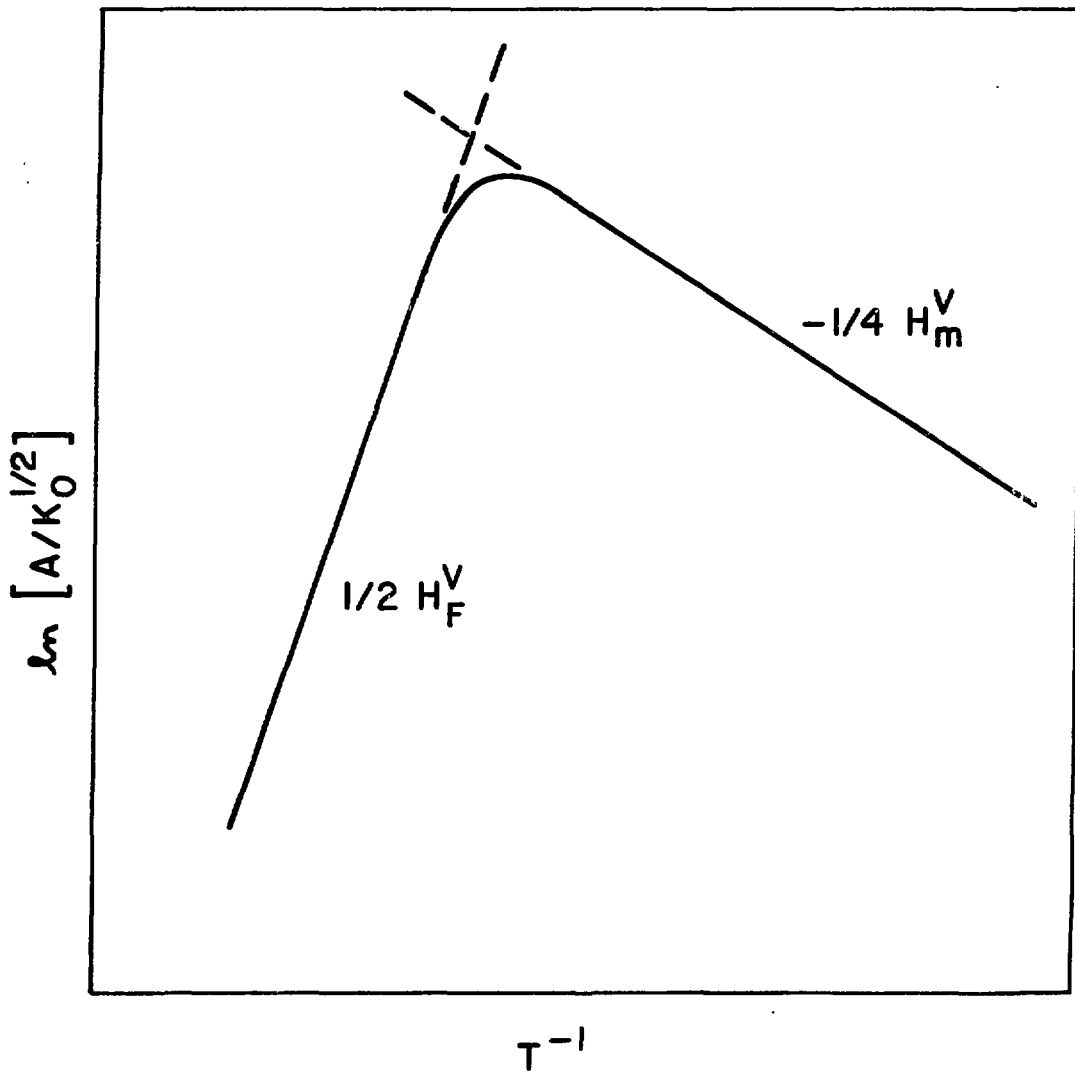Table 1. Relative Efficiencies and Peak Segregation Temperatures

| particle | | $K_c$ (dpa/s) | $(\varepsilon/a_r)$ | T(K) (num) | T(K) (Eq. 8) | $\varepsilon/\varepsilon_p$ (num) | $\varepsilon/\varepsilon_p$ (Eq. 14) |
|---|---|---|---|---|---|---|---|
| 1.0 MeV | H | $2.6 \times 10^{-5}$ | $1.51 \times 10^{-3}$ | 818 | 818 | 1.00 | 1.00 |
| 2.0 MeV | He | $2.6 \times 10^{-5}$ | $7.14 \times 10^{-4}$ | 808 | 810 | 0.47 | 0.48 |
| 2.0 MeV | He | $3.1 \times 10^{-4}$ | $7.14 \times 10^{-4}$ | 843 | 843 | 0.50 | 0.50 |
| 2.0 MeV | Li | $3.1 \times 10^{-4}$ | $5.56 \times 10^{-4}$ | -- | -- | 0.37 | -- |
| 3.0 MeV | Ni | $6.9 \times 10^{-4}$ | $1.19 \times 10^{-4}$ | 828 | 828 | 0.08 | 0.08 |
| 3.25 MeV | Kr | $3.1 \times 10^{-4}$ | $1.59 \times 10^{-5}$ | -- | -- | 0.01 | -- |

References

[1]    P. R. Okamoto, L. E. Rehn and R. S. Averback, J. Nucl. Mater. 108-109 (1982) 319.

[2]    L. E. Rehn, P. R. Okamoto and R. S. Averback, Phys. Rev. B 30 (1984) 3073.

[3]    D. I. Potter, L. E. Rehn, P. R. Okamoto and H. Wiedersich, St. Metall. 11 (1977) 1095.

[4]    L. E. Rehn, R. S. Averback and P. R. Okamoto, Advanced Techniques For Characterizing Microstructures, eds. F. W. Wiffen and J. A. Spitznagel (AIME, Warrendale, PA, 1982) p. 269.

[5]    R. S. Averback, L. E. Rehn, W. Wagner, H. Wiedersich and P. R. Okamoto, Phys. Rev. B 28 (1983) 3100.

[6]    T. Moroga, P. R. Okamoto and H. Wiedersich, Radia. Eff. Lett. 68 (1983) 163.

[7]    H. Wiedersich, Radia. Eff. 112 (1982) 111.

[8]    P. R. Okamoto, L. E. Rehn, R. S. Averback, K. M. Robrock and H. Wiedersich, in:  Point Defects and Defect Interactions in Metals, eds. J. Takamura et al. (University of Tokyo Press, Japan, 1982) p. 946.

[9]    N. Q. Lam, S. J. Rothman and R. Sizemann, Radia. Eff. 23 53.

[10]   R. S. Averback, R. Benedek and K. L. Merkle, Phys. Rev. B 18 (1978) 4156.

**Figure Captions**

Fig. 1.  Schematic Arrhenius plot of the predicted temperature dependence for

coating growth.

Fig. 2.  Arrhenius plot of the measured parabolic growth-rate constants for

$Ni_3Si$ coatings on Ni-12.7 at.% Si alloys for different ion

irradiations.

Fig. 3.  Relative efficiencies of various ions for producing mobile defects

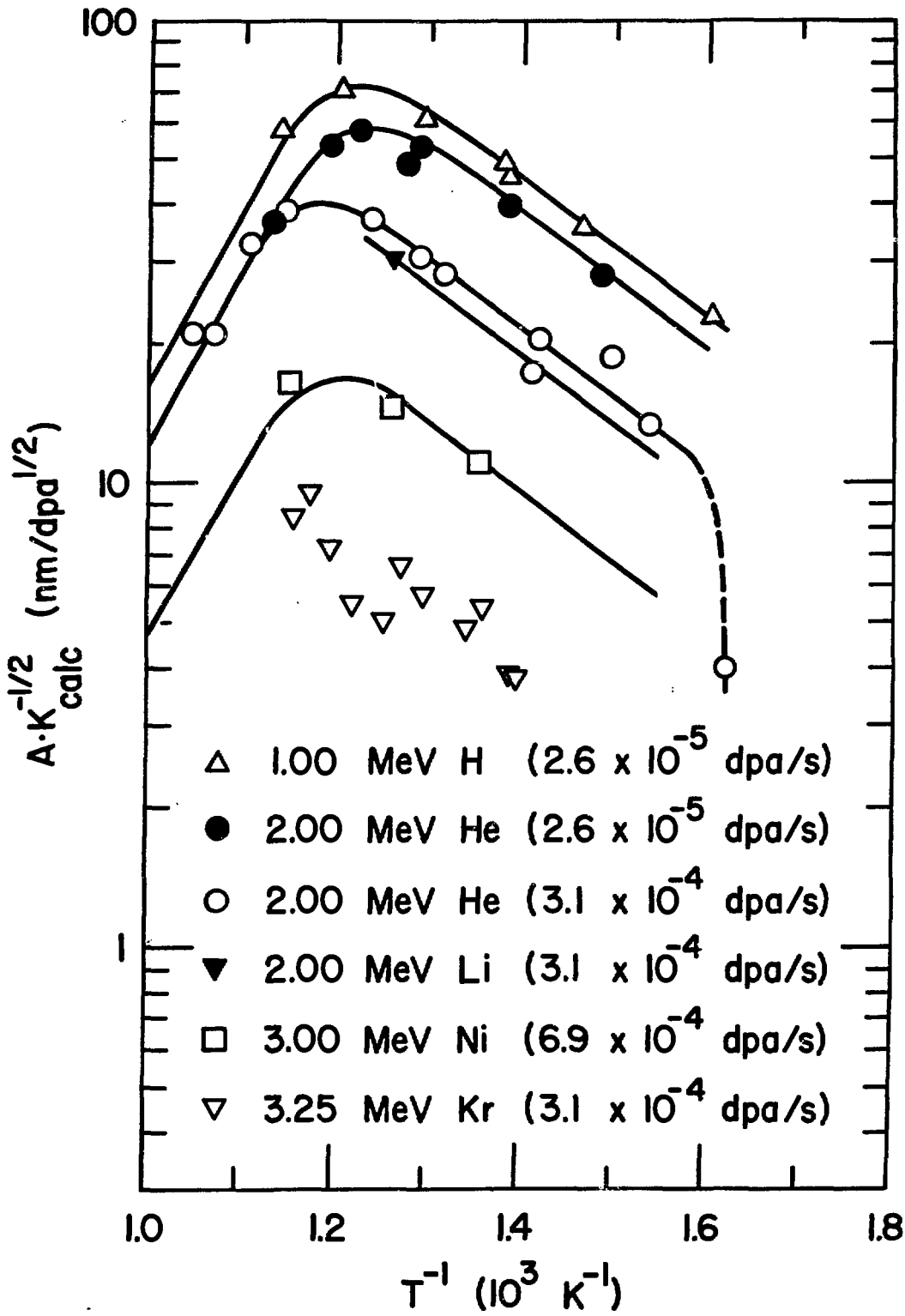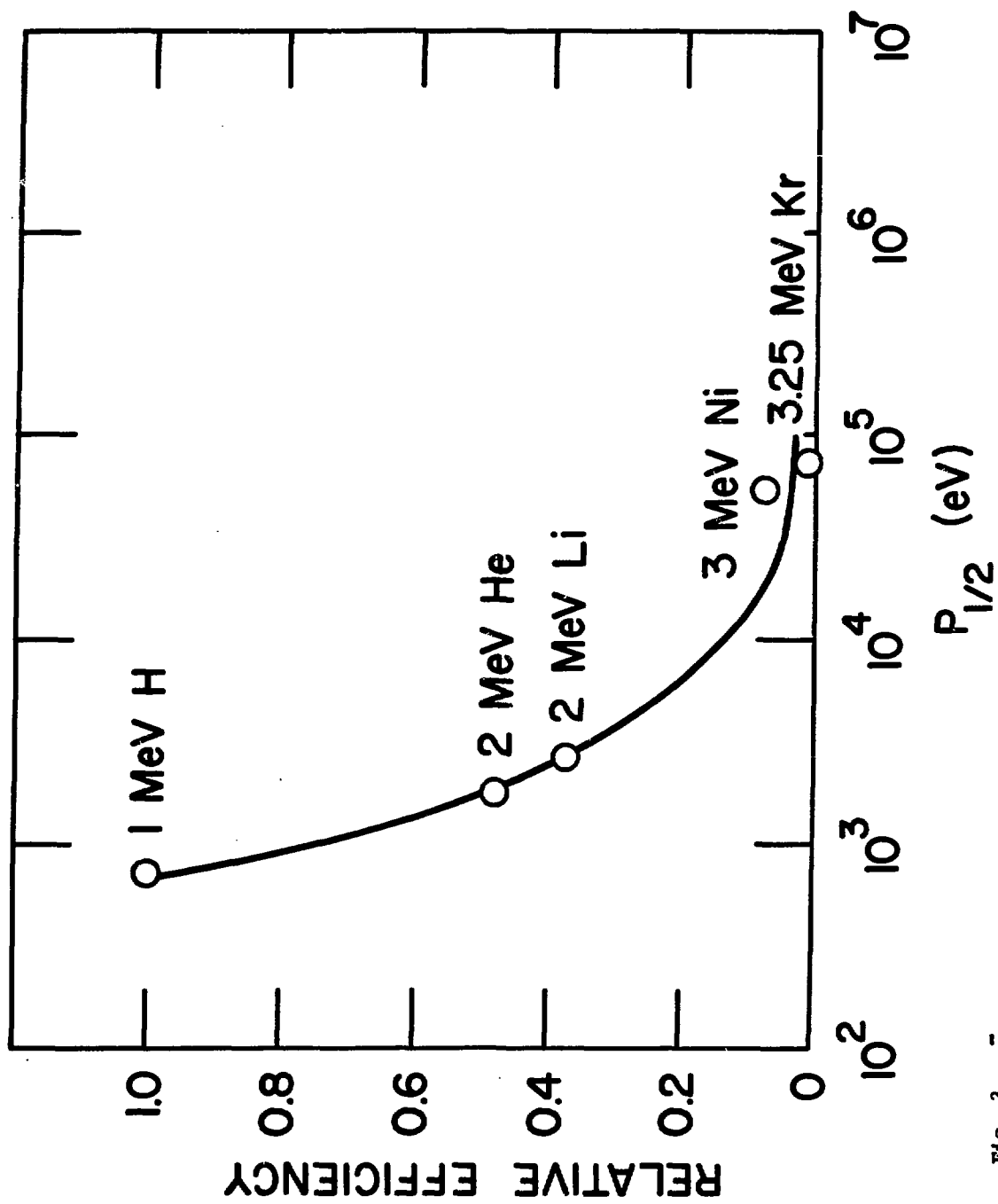plotted as a function of the weighted-average recoil energy.

Fig. 1

Fig. 2

Fig. 3